Title

Creative use of analytical techniques and high-throughput technology to facilitate safety assessment of engineered nanomaterials

Journal

Analytical and Bioanalytical Chemistry, 410(24)

ISSN

1618-2642

Authors

Liu, Qi
Wang, Xiang
Xia, Tian

Publication Date

2018-09-01

DOI

10.1007/s00216-018-1289-y

Peer reviewed

HHS Public Access

Author manuscript

Anal Bioanal Chem. Author manuscript; available in PMC 2019 September 01.

Published in final edited form as:

Anal Bioanal Chem. 2018 September ; 410(24): 6097–6111. doi:10.1007/s00216-018-1289-y.

Creative use of analytical techniques and high throughput technology to facilitate safety assessment of engineered nanomaterials

Qi Liu[1,2,#], **Xiang Wang**[1,2,#], and **Tian Xia**[1,2,3,*]

[1]Center of Environmental Implications of Nanotechnology (UC CEIN), University of California, Los Angeles, CA 90095, USA

[2]California NanoSystems Institute, University of California, Los Angeles, CA 90095, USA

[3]Division of NanoMedicine, Department of Medicine, University of California, 570 Westwood Plaza, Los Angeles, CA 90095, USA

Abstract

With the rapid development and numerous applications of engineered nanomaterials (ENMs) in science and technology, their impact on environmental health and safety should be considered carefully. This requires an effective platform to investigate the potential adverse effects and hazardous biological outcomes of numerous nanomaterials and their formulations. We consider predictive toxicology a rational approach for this effort, which utilizes mechanism-based in vitro high-throughput screening (HTS) to make predictions on ENMs adverse outcomes in vivo. Moreover, this approach is able to link the physicochemical properties of ENMs to toxicity that allows the development of structure activity relationships (SARs). To build this predictive platform, extensive analytical and bioanalytical techniques and tools are required. In this review, we described the predictive toxicology approach and the accompanying analytical and bioanalytical techniques. In addition, we elaborated several successful examples as a result of using the predictive approach.

Keywords

engineered nanomaterials; predictive toxicological paradigm; analytical technique and bioanalytical assays; high throughput screening; nano-structure activity relationships

1. Introduction

Advances in nanotechnology represented by engineered nanomaterials (ENMs) have opened a new era for nanomaterials in material design and application. The unique properties of ENMs, i.e., large specific surface area, shape, crystalline structure, and surface chemistry,

*Corresponding author, txia@ucla.edu.
#Qi Liu and Xiang Wang contributed equally to this work.

Compliance with Ethical Standards

Conflict of interest: The authors declare that they have no competing interests.

endow them with new functions. This is the reason that ENMs have been increasingly and widely used into various aspects of our daily lives such as electronics [1], lithographic techniques [2], catalysis [3], cosmetics [4], medical devices [5], drug delivery systems, and vaccines [6]. Even though enormous excitements and expectations have emerged regarding their applications, the rapid development and commercialization of ENMs increase potential risks (e.g., toxic effects) and this has generated grave concerns in the society. These effects, mainly hazardous biological outcomes, will be related to their unique physicochemical properties [6]. However, to evaluate considerable number of ENMs and investigate their possible adverse effects is a major challenge. Reliable and efficient methods and techniques are needed. To date, this information is often scattered and there is a need for a review that covers majority of the analytical techniques for nanotoxicological studies. Based on the eventual interactions between ENMs and cells taking place at the nano/bio interface, the toxicological studies should be tested at the biomolecular and cellular level, followed by essential in vivo animal validation experiments for the relevance of the in vitro studies [7]. This review will cover the novel platform (Figure 1), defined as predictive toxicological paradigm, through the use of high throughput screening (HTS) and structure-activity relationship (SAR) based mechanism in vitro studies [7]. We will highlight the analytical and bioanalytical techniques that are quite essential for predictive toxicology of nanomaterials. This approach includes the establishment of systematic ENM library, the in vitro cellular or bio-molecular injury mechanisms capable of predicting potential human and environmental hazard, and validation by limited animal studies [8]. Theses robust scientific paradigms, characterized by screening of multiple toxicants concurrently, was recommended to be an alternative testing approach to reduce costly animal studies examining one toxicant at a time [8]. Consequently, this platform will facilitate design of safer ENMs for sustainable development of nano-applications.

2. Fundamental elements to establish a predictive toxicological paradigm

Four elements were necessary for establishing this predictive toxicological paradigm: (1) synthesis of compositional and combinational ENM libraries; (2) comprehensive physicochemical characterizations of ENMs; (3) use of in vitro high content and rapid throughput screening method and platform to assess the biological effects of nanomaterials and their related properties with the goal to link the properties to biological injury, and (4) validation of in vitro prediction through limited but focused in vivo studies to establish SARs.

2.1 Build compositional and combinatorial ENM libraries

ENM libraries are essential for toxicity screening and understanding the role of their properties in adverse outcomes [9]. The selection of ENMs for study should consider the commercial production volume of ENMs and their potential exposure to human and environment. To investigate the biological effects of ENMs, two major types of ENM libraries need to be prepared (Figure 2). One is compositional library that are different in chemical compositions, e.g., metal, carbon, silica, metal oxide, rare earth NPs, etc. Recently, a library of NPs made of different combinations of five different metals were synthesized using dip-pen lithography. This multimetallic library include 31 different particle

combinations of gold, silver, copper, and nickel [10]. The other is combinatorial library that is composed of ENMs that vary in (ideally) one major property while other properties are largely same, e.g., aspect ratio, size, charge, dissolution rate, surface functionalization, crystallinity, etc.[11–16]. For example, Ji et al. synthesized a serious of cerium oxide (CeO_2) nanorods and nanowires with precisely controlled lengths and aspect ratios. The successful creation of a CeO_2 combinatorial library allowed the systematic in vitro cellular study of the effect of aspect ratio on lysosomal damage, cytotoxicity, and IL-1β production [12, 17]. Xia et al. synthesized a batch of iron-doped ZnO with different dissolution rates, and demonstrated decreased dissolution of ZnO by iron doping yielded nanoparticles with reduced toxicity in the rodent lung and zebrafish embryos [18]. By using reduction or hydration of pristine graphene oxide, Li et al. prepared a graphene oxide library varying on surface oxidation states, and determined the carbon radicals are responsible for membrane damage, lipid peroxidation, and cytotoxicity in macrophages in a pulmonary toxicity model [19]. Other examples of combinatorial library includes highly purified metallic and semiconducting single-walled carbon nanotubes (SWCNTs) [20], and covalently functionalized multiwall carbon nanotubes (MWCNTs) with different surface charge [21]. The quality of the compositional and combinatorial libraries is important for us to link physicochemical properties of ENMs to their adverse outcomes and build SARs.

2.2 Physicochemical characterizations of ENM libraries

Typically, compared with small molecules and bulk materials, nanomaterials had distinct physicochemical properties, especially in size, surface charge, shape, composition, chemical/physical structure, colloidal/chemical stability, dispersion and surface properties. These properties were critically relevant to particular physiological interactions, which would cause subsequent adverse outcomes or toxicity. For any given ENM, three major categories of physicochemical properties were identified in extensive studies from the literature: (1) intrinsic (as-produced) properties, such as chemical composition, primary size (size distribution), shape, chirality, crystallinity, and purity; (2) extrinsic properties such as properties that are acquired after ENM dispersion in biological fluid or media during storage or usage, e.g., surface charge, dispersion state, agglomeration size or kinetics, and dissolution rate; (3) emerging properties that are responsible for toxicological outcomes obtained during biological experimentation and SAR analysis, e.g., adsorption of phosphate on rare earth particles, display of surface silanol and siloxane groups on silica particle surfaces, or carbon radicals on graphene oxide surfaces. In this context, it is important to understand how the different physicochemical characteristics of nanomaterials affect their behavior and toxicity [22, 23]. This demands reliable and robust techniques for determining the different physicochemical characteristics of nanomaterials. A list of main techniques and assays, used for characterization of the three groups of ENMs properties as well as appropriate analytical tools are described in Table 1. A tiered process to efficiently characterize one newly acquired material was recommended by starting with a set of basic characterization, such as the intrinsic properties and some of the extrinsic properties including surface charge, dispersion state, agglomeration size in the biological fluid, supplemented by additional characterization of relevant extrinsic or emerging properties according to the SAR analysis process. A rigorous but practical approach to reliable characterization is essential for understanding nanoparticle toxic potential.

2.3 Develop robust mechanism-based in vitro high throughput screening (HTS) assays to quantitatively assess cellular injury responses linking to ENM's physicochemical properties

After preparation of ENM libraries and determination of ENMs' physicochemical properties, the next step is to build the relationship between these properties and their cellular injury responses. Compared to in vivo studies, cellular assays can be performed in high throughput format that allow toxicity screening to many ENMs in multiple doses and time points. Most importantly, in vitro assays could be selected to reflect a specific toxicological pathway or mechanism of toxicity, which is the major link between in vitro and in vivo toxicity outcomes. Although there are major differences in terms of toxicity endpoints between in vitro and in vivo, the mechanism of toxicity is the intrinsic connection between the two models. Based on the availability of various mechanism-based in vitro assays, we advocate to use these assays, wherever possible, in high throughput format, to perform in vitro toxicity screening with the goal to link in vitro toxicity with pathological effects in vivo. Currently, there are major mechanistic pathways of toxicity have been linked to ENM toxicity, which include injury paradigms such as frustrated phagocytosis, the generation of reactive oxygen species (ROS) and oxidative stress, pro-/anti-inflammatory cytokine production, lysosomal and autophagy dysfunction, membrane peroxidation and damage, apoptosis, necrosis, pyroptosis, etc. [25]. These endpoints could be assessed utilizing various assays/techniques in Table 2. The screening of ENMs' biological impact on various cells could be undertaken to capture each stage (endpoint) of the cells, including cell viability, cell uptake (phagocytosis, endoycytosis, micropinocytosis, etc.), as well as integrity of phagolysosome function, oxidative stress, pro- and anti-inflammatory responses, lysosomal dysfunction and NLRP3 inflammasome activation, and autophagy disruption.

The earlier HTS technologies usually bring large amounts of false-positive and false-negative results due to the lack of consideration for "dose-response" relationship. This is contrary with the basis of most molecular interactions in biological systems, and that limits HTS to be applied to the identification in the field of subtle, complex pharmacology, such as partial agonism or antagonism [26, 27]. Therefore it is necessary to generate dose-response curves using a quantitative primary screen, or the follow-up of a single-point screen [26, 28]. Researchers developed a new screening system based on the use of droplets in a microfluidic system creating and manipulating picoliter-volume aqueous droplets that function as independent microreactors during drug screening [26, 29]. As a result of the miniaturization inherent in this approach, their system was capable of generating high-resolution dose-response curves containing approximately 10,000 datapoints, resulting in extremely precise measurement of dose-response relationships using minimal quantities of reagents [29].

It is essential to determine the accurate and precise dose metrics of delivered ENMs for the meaningful and reproducible in vitro HTS cellular assays. The typical computational modeling approaches to determine the cellular dose of ENMs are in vitro sedimentation, diffusion and dosimetry (ISDD) model, volumetric centrifugation-in vitro sedimentation, diffusion and dosimetry (VCM-ISDD) model, and (distorted grid) DG model [30–33]. Hinderliter et al. developed ISDD model of soludion particokinetics (sedimentation, diffusion) and dosimetry for non-interacting spherical particles and their agglomerates in

monolayer cell culture systems [34]. ENMs' transportation to cells could be calculated by simultaneous solution of Stokes Law (sedimentation) and the Stokes-Einstein equation (diffusion) [34]. By using ISDD model, the effects of particle size, particle density, agglomeration state and agglomerate characteristics could be studied on cell dosimetry in vitro [34]. The researchers put the VCM effective density into the ISDD model, and this generated VCM-ISDD model [32]. The newly-developed one-dimensional DG model could estimate delivered ENM dosimetry and emulate the biokinetics at the particle-cell interface using a Langmuir isotherm, governed by a user-defined dissociation constant, K_D, and allow modeling of ENM dissolution over time [31]. Measurement of the delivered cellular dose of ENMs could be achieved feasibly using various kinds of microscopy when ENMs are labelled. Besides the theoretical model mentioned above, analytical ultracentrifugation (AUC), still remains the gold standard to directly measure effective ENM cellular density. The challenges which hinder the broad use of AUC is the relative high cost and low throughput. DeLoid et al. recently developed the volumetric centrifugation method (VCM), a rapid and inexpensive method to accurately measure the effective density of nano-agglomerates in suspension [35]. This method use a packed cell volume (PCV) tube to obtain the volume of the pellet (in the capillary section of PCV tube) from benchtop centrifugation of ENM suspension. Based on the measured volume of the pellet and known volume of ENM, the effective density can be calculated as a weighted average of media and ENM [36]. And the authors validated their data against the results from AUC. The dosimetry of ENMs still remains a big challenge, and it calls for the development of reliable and efficient methods towards the further toxicological testing and investigation of in vitro nano-bio interactions.

Most nanotoxicity studies chose to study cell viability or cell death in vitro in different cell lines. However, there is poor connectivity between cell viability and in vivo adverse outcomes, especially for long term effects. This is due to the cell viability assays seldom offer mechanistic insights, which is the intrinsic connection between in vitro and in vivo. However, cell viability assays are still useful as a first step of toxicity screening to create a separation between potential high-toxicity and low-toxicity ENMs. For ENMs with high toxicity, additional assays are needed to understand the mechanisms of toxicity. While for low toxicity ENMs, alternative assays such as pro-inflammatory effects are needed to determine their potential toxic effects. The typical cell viability markers measure a biochemical event that occurs in living cells but stops after cell death. Indicators that undergo a quantity change as a result of toxicity have been proven to be useful as markers of cell viability. Cell viability can be measured by the quantitation of adenosine 5′-triphosphate (ATP), 5-(3-carboxymethoxyphenyl)-2-(4,5-dimethylthiazolyl)-3-(4-sulfophenyl) tetrazolium (MTS) reduction, and release of lactate dehydrogenase (LDH), as markers for cells with a compromised ATP production, cellular reduction potential, and membrane integrity, respectively [58]. Subsequently, a number of different reagents and indicator dyes have been developed to increase the throughput of cell viability assays. George et al. demonstrated ZnO nanoparticles were capable of ROS generation and activation of an integrated cytotoxic pathway which includes intracellular calcium flux, mitochondrial depolarization, and plasma membrane leakage [38]. These responses could be assessed contemporaneously using fluorescent dyes by a semi-automated epifluorescence procedure.

These multi-parametric assays have been demonstrated to have great potential for ENM toxicity screening [38].

Oxidative stress is the most studied toxicity mechanism for chemicals and ENMs, which should be quantitatively measured by cellular assays. There are many popular assays available for detecting oxidative stress. A change in cellular GSH levels is the main indicator of oxidative stress, which could lead to a range of cellular responses, from antioxidant defense, pro-inflammatory effects, to apoptosis or cell death. The GSH-Glo Assay is a luminescent-based assay for the detection and quantification of glutathione (GSH) in cells. The assay is based on the conversion of a luciferin derivative into luciferin in the presence of GSH. The reaction is catalyzed by a glutathione S-transferase (GST) enzyme that is supplied in the kit [37]. There are also fluorescent dyes that could determine the intracellular sources of ROS. MitoSOX reagent is a fluorogenic dye specifically targeted to mitochondria in live cells. Oxidation of MitoSOX reagent by ROS produces red fluorescence [59]. CellROX is also a novel fluorogenic probe for measuring cytoplasmic oxidative stress in both live and fixed cells, with absorption/emission maxima at ~644/665 nm [60]. The cell-permeant dye is non-fluorescent while in a reduced state, and exhibits bright fluorescence upon oxidation by ROS. The Image-iT Lipid Peroxidation Assay enables the detection of lipid peroxidation in live cells through oxidation of BODIPY 581/591 C11 reagent, which will display a shift in peak fluorescence emission from ~590 nm to ~510 nm. Fluorescence from live cells shifts from red to green, providing a ratiometric indication of lipid peroxidation [19, 61]. These assays provide simple and sensitive approaches and can be adapted easily to high-throughput applications.

For some ENMs, although they have no obvious effects on cell viability, they could induce pro-inflammatory effects by secretion of cytokines, which influence cell functions and injury mechanisms. Typically, pro-inflammatory responses (as a result of NF-κB and AP1 activation) and anti-inflammatory cytokines (IL-10, TGF-β1) should be determined. For protein quantification, especially cytokine detection, the enzyme-linked immunosorbent assay (ELISA) has been a gold standard method since first introduced in the early 1970s. Building upon the ‘sandwich’ ELISA concept, the multiplex assay utilizing antibody-conjugated microspheres (‘beads’) form Luminex has been established [62]. The unique multiplexing capabilities of the Luminex assays are based upon the use of magnetic microspheres that have been internally dyed with red and infrared fluorophores of differing intensities. Each bead is given a unique number, or ‘bead region’, allowing differentiation of one bead from another. Individual bead sets are coated with a capture antibody qualified for one specific analyte. The captured anaylte from a sample is detected using an analyte-specific biotinylated antibody that binds to the appropriate epitope of the immobilized analyte, plus streptavidin-conjugated R-phycoerythrin (SA-RPE) [63]. Beads coated with different antibodies can be mixed in the same assay, utilizing a 96-well microplate format. The instrument, like Luminex detection system, could differentiate bead color, for the specific analyte, and RPE fluorescence intensity to quantify the analyte captured by the bead. Bio-Plex technology (BioRad based on Luminex xMAP technology) is a bead-based technology with its potential to serve as an alternative diagnostic tool to conventional methods currently used such as ELISA and RT-qPCR. Similar to enzyme-linked immunosorbent assay, Bio-Plex uses up to 100 color-coded fluorescent bead sets, containing

different ratios of two spectrally distinct fluorophores, making each bead set distinguishable by its fluorescent emission when excited by a laser. Each bead set can be conjugated with a unique protein, peptide, oligonucleotide or antibody. Coupled beads are then incubated with a sample in a 96-well ELISA plate format, followed by incubation with a biotinylated antibody using streptavidin-phycoerythrin as the reporter. The assay is then read on a Bio-Plex reader. Fluorescent intensity of the reporter conjugate is then measured to determine the quantities of target analytes in samples, and the reading intensity of the fluorescence is proportional to the amount of analytes in the samples. The Bio-Plex immunoassay has many advantages, such as high specificity, high throughput, quantitative assay and easy-to-use 96-well plate-based suspension analysis system [64, 65]. Microarray printed immune-capture multiplex assays such as Quansys Q-Plex ™, based on 96-well plates wherein up to 25 different capture antibodies have been printed on each well surface, allow for quantification of up to 25 unique cytokines from single 5-30 μL samples [66]. Another novel alternative technique to ELISA is AlphaLISA bead-based technology, which is developed based on luminescent oxygen-channeling chemistry [67]. AlphaLISA assays eliminate the need for multiple washes to separate bound from unbound assay components. And they are performed following simple ‘mix-and-measure’ protocols with reduced hands-on and total assay times [68]. AlphaLISA assays are truly miniaturizable and automatable with sample volumes as low as 1 μL in total assay volumes of 10 μL in 96-, 384- or even 1,536-well-plate format [69]. They can exhibit remarkable sensitivity, wide dynamic range and robust performance compared to ELISA [68]. Flow cytometry is also a useful technique in cellular assay, and is significantly capable of sorting free particles, particle aggregates, cell-associated particles, and particle-free cells, which allow for the assessment of fractions of cells that associate with particles if the particles are intrinsically fluorescent or can be tagged post-facto with fluorescence [70–73]. Aside from Luminex assays, recent application of flow cytometry instrument, based on multiplexed cytometric bead assays, namely CBA, has been employed for exploiting libraries of various fluorescent bead-linked antibodies for the simultaneous detection of 30 or more cytokines [74].The Luminex, Microarray and AlphaLISA based assays have become powerful and cost-effective tools for the simultaneous measurement of multiple cytokines in samples with limited volumes.

Cell visualization, including phagocytic activity, internalization, and organelle interaction, could be monitored by microscopy. High-resolution inspection of chemically fixed and carefully desiccated cell samples by TEM — its high-resolution (HR-TEM) and energy-filtering (EF-TEM) embodiments — can reveal organelle-nanomaterial interactions that my help to elucidate nanomaterial-specific mechanisms of cellular toxicity [76, 77]. Cell-nanomaterial interactions observed by TEM include differentiation of cytosolic free-floating aggregates from membrane-bound aggregates. For example, we observed the transformation of spherical rare earth oxides (REO) to sea-urchin shaped structures inside lysosomes by TEM [56]. Additionally, Confocal Laser Scanning Microscopy (CLSM) fluorescence microscopy have also been used to image particle uptake and internalization within cell organelles (e.g., endosomes, lysosomes) or autophagy disruption [78]. For example, we studied the lysosomal membrane damage by Magic Red cathepsin B substrate staining, which formed punctate staining pattern in intact lysosomes, however, cells with damaged lysosomes showed a diffuse staining pattern in the cytosol [56]. Moreover, CLSM offers

accessibility of pseudo-3D images through image reconstruction algorithms combining several axial and lateral images [77].

ENMs induced cellular injuries, e.g., oxidative stress, generally involves tiers of responses including cellular antioxidant defense, activation of pro-inflammatory signaling pathways leading to the production of cytokines/chemokines, and then final mitochondria-mediated cell death [38, 79–81]. Typically, two to three weeks' effort is required to perform the entire panel of the three tiers of oxidative stress responses. HTS approach could not only speed up this process, but also provide various advantages over conventional assays [82, 83]. First, HTS could establish the standardization of the procedure, offer automation of the assay, such as, cell seeding, liquid handling, imaging, image analysis, etc., and miniaturization which would require less amounts of reagents and lower the cost per assay. Second, HTS is capable of screening large ENM libraries, and also it can be utilized for different cell lines, time points and doses in the concurrent experiment, which decrease the inter-experiment variations. Third, with the assist of computer and related software, HTS could facilitate the development of SARs based on large data sets. As an example of such an assay, we have developed a multi-parametric and high throughput screening procedure that incorporates cellular oxidative stress responses involved in the advanced level of oxidative stress (Figure 3)[38]. These approaches speed up the rate of ENM hazard assessment and allow the development of nano-structure-activity (nano-SARs) and hazard ranking of ENMs.

3. Successful case studies of using predictive toxicology paradigms and HTS approach

In this part, we will review five aspects of mechanism-based paradigms using established HTS approach and predictive toxicology paradigms (Figure 4). The first example is the study of toxicological profile of metal oxide (MOx) nanoparticles[39]. Researchers have previously demonstrated via single or a small number of NP explorations that many types of MOx nanoparticles can generate oxygen radicals and induce oxidative stress, which plays the role in their ability to induce toxicity in mammalian cell lines and in vivo [84–86, 38, 49]. Rushton et al. found that compared to TiO_2 and gold NPs, copper NPs had the greater activity to produce ROS in both cell-free and cellular assays [84]. Cho et al. applied their rat model and studied various types of infiltrating cells, time period, cytotoxicity, and inflammatory mediators to characterize the different types of ROS-related inflammation induced by four metal oxide NPs (CeO_2, NiO, ZnO, and CuO) [85]. The mechanisms for generating the oxidative stress are due to the facts that these MOx nanoparticles can serve as conduits for electron transfers between aqueous reactants and these transfers are dependent on similarities in the energetic states of the NPs and the biological redox-active substances. While the relevant energy levels for the semiconductor are the top of the valence band (Ev) and the bottom of the conduction band (Ec), the relevant energy level for aqueous substances is their standard redox potential (E0) [19]. Burello and Worth have suggested a theory in which the relationship between the biological redox potential to MOx band gap could explain the oxidative stress and toxicity induced by the NPs [21, 22]. More specifically, it is suggested that the overlap between Ec and/or Ev with biological redox potentials ranging from −4.12 to −4.84 eV promoted electron transfer and lead to reactive radical production

and oxidative stress injury. In order to demonstrate this hypothesis, it is necessary to study a number of representative MOx NPs simultaneously, which requires a more efficient strategy, i.e. the HTS, to fulfil the task. Accordingly, 24 representative metal oxides were chosen with high quality and similar primary sizes in the range of 10-100 nm. Band gap energy was measured by UV-vis spectroscopy, and absolute electronegativities (χ_{oxide}) were calculated using a set of equations reported by Portier et al. [87]. The characterization of Ec and Ev values confirmed that the Ec of CoO, Co_3O_4, Cr_2O_3, Mn_2O_3, Ni_2O_3, overlapped with the cellular redox potential, which is supposed to induce adverse outcomes. The multi-parameter HTS was conducted on these metal oxides in macrophages and bronchial epithelial cells at a wide concentration range (from 0.375 to 200 μg/mL) hourly, which demonstrated that the overlap was indeed well correlated with the ability of these MOx nanoparticles to induce ROS generation, oxidative stress, and pro-inflammatory responses. To confirm this hypothesis, effects of the nanoparticles on a representative redox couple, cytochrome c-Fe^{3+}/ cytochrome c-Fe^{2+}, were studied by spectroscopic methods. The results demonstrated that among the MOx nanoparticles showing Ec overlap with the cellular redox potential were capable of oxidizing cytochrome c. In addition, it was found that CuO and ZnO were toxic but their Ec values are outside the biological redox potential range, this is because dissolution and shedding of toxic ions play a key role in their toxicity. The in vivo experimental results mirrored the in vitro outcomes in the animal lung, which demonstrated that this in vitro multi-parameter HTS approach predicted pro-inflammatory potential in the lung. To understand the integrated relationship of Ec and Ev to the biological redox potential, a library of Co_3O_4 nanoparticles was established with incremental PdO doping, which created heterojunctions to adjust Ec and Ev levels. The PdO doping allowed electron capture from the redox couples that maintain the biological redox potential, causing disruption of cellular redox homeostasis and induction of oxidative stress. These PdO/Co_3O_4 nanoparticles significantly increased the generation of oxidant injury and inflammation. [88]Altogether, it is feasible to establish a predictive toxicological paradigm for MOx toxicity based on their conduction band energy and dissolution rate.

The second example is the toxicity assessment for SiO_2 nanoparticles [89, 50, 90], one of the most produced nanomaterials worldwide in industry, which have been widely used in cosmetics, sunscreens, catalysts, textiles, and solar batteries. SiO_2 could be grouped by their crystallinity into crystalline (e.g., quartz) and amorphous (e.g., high-temperature flame pyrolysis to form fumed or pyrolytic silica, or under hydrothermal conditions to form precipitated, colloidal, or mesoporous silicas). Although quartz are known for causing silicosis and silica-related diseases [91], amorphous SiO_2 are generally considered as safe (GRAS) by FDA. However, recent evidence showed that amorphous silica could also cause toxicity in vitro and in vivo, thus it is important to establish SARs to understand the mechanism of toxicity induced by amorphous silica. Compared to crystalline silica with well-defined structure, amorphous silicas, with a flat energy landscape, do not have long-range order, and will change with the environmental factors [92]. Moreover, they have high surface area, which might produce large amount of surface radicals [93]. In spite of numerous previous studies of their toxicity leading to silicosis and chronic inflammation [94, 95], their toxicological behaviors remain less well understood due to their diverse structures. Many researchers documented amorphous slilicas' toxicity to lysis red blood

cells without regard to their framework and surface chemistry, and thus colloidal, biomolecular, and toxicological behaviors [96–101]. Therefore, detailed characterization of physicochemical properties of amorphous silicas and systemic mechanism studies of those properties variation are highly needed [102, 9]. The amorphous silica framework and surface chemistry, in particular the hydroxyl (silanol) coverage and size and distribution of siloxane rings, exhibit a wide range of configurations. Specifically, Zhang et.al compared the toxicity of fumed silica with colloidal stöber silica, and found that fumed silica is extremely toxic while stöber silica has low cytotoxicity. Additional experiments demonstrated that fumed silica cytotoxicity could be attributed to the surface display of silanol groups [89]. The density of surface silanol groups (≡Si-OH) determined the interaction between the silica surface and membrane phospholipids, which lead to membrane perturbation and hemolysis of red blood cells. Moreover, the cleavage of strained three-membered rings (3MRs)at the fumed silica surface was the generation of hydroxyl radicals, which could further enhance the membrane perturbation and generation of danger signals that lead to the assembly of the NLRP3 inflammasome. This SAR was developed by using FTIR to determine silanol group concentrations, Raman spectroscopy to measure the ring concentration, and abiotic ROS generation assays using fluorescent dyes such as DCF. Therefore, it was found that the key characterizations to establish the predictive paradigm for SiO_2 nanomaterials was to determine the strained (3MRs) and surface display of silanol groups on different types of amorphous silica. Meanwhile, this information could also be used to develop the safe-by-design strategy through surface modification to reduce the 3MRs as well as surface density of silanol groups. In particular, by using a library of calcined and doped fumed silica nanoparticles, the HTS demonstrated that calcination and rehydration are the two simple and effective treatments to reduce the toxicity of fumed silica. While calcination could reduce the surface silanol content via condensation (e.g., ≡Si–OH + HO-Si≡ ⇔ ≡Si–O–Si≡ + H_2O), doping by flame spray pyrolysis (FSP) with certain inert metals, e.g., aluminum (Al) or titanium (Ti), offered a one-step approach for the synthesis of homogeneous and high-purity nanomaterials, both of which could decrease the surface reactivity of fumed silica by reducing the surface concentration of the hydrogen-bonded vicinal silanol groups [50, 90]. There are also studies which demonstrated that the physicochemical properties of SiO_2 nanomaterials determine their toxicity [103–105]. In summary, it was observed that reduction in surface silanol display could be effective at reducing acute lung inflammation and pro-inflammatory effects in vitro. This demonstrated the possibility of a safer-by-design approach for fumed silica.

The third example is the work with the engineered carbonaceous nanomaterials (ECNs), which includes carbon nanotubes (CNTs), graphene and graphene oxides (GO) [20, 21, 106–109]. These materials have intrinsic electrical and optical characteristics, as well as the capability to finely tune the physicochemical properties such as size, durability, and surface chemistry, facilitating them to be widely used in biomedical and electronics industry. Limited by their low solubility and dispersibility in both organic and inorganic solutions [110], CNTs are usually modified by surface functionalization via noncovalent and covalent approach. Noncovalent ways include surface coating with amphiphilic molecules and surface binding of solvophilic molecules. Covalent methods, involving terminal carboxylation (such as amine, polyethylene glycol, and polyetherimide derivatives) and

sidewall modification (e.g. sidewall-NH_2) of the tube surface, can be better controlled and more stable [111–116]. The rapid growth of CNT and their functionalized derivatives has necessitated the studies of the accompanying adverse effects. In order to comprehensively compare tubes with different characteristics, it is necessary to develop predictive toxicology paradigms which could characterize and categorize CNTs, graphene, GO into the specific libraries based upon their unique properties, for example, CNTs of different synthesis methods, dispersal states, surface functionalization, and lengths, etc. [106–109, 117]. The key characterization methods are listed in Table 1. In particular, by studying a CNTs library at different surface functionalization, it was demonstrated that the pristine (nonfunctionalized), hydrophobic, and positively charged (e.g., polyetherimide [PEI]-modified) CNTs generate pro-fibrogenic effects in vitro and in animal lungs, whereas the hydrophilic or negatively charged (e.g., COOH- or PEG-modified) CNTs have less or no toxic effects [21]. A recent report showed NH_2-CNTs led to increased pulmonary collagen deposition along with increased production of TGF-β1 and IL-6 [118]. While researchers also showed that surface charge determined the fibrogenic potential of CNTs, however there were some properties that did not play an independent role in the chronic effects in the lung. For example, the chirality or electrical property is another unique characteristic of SWCNTs, which is important in its applications in areas of electronics, optics, and sensing, etc. Based on the chirality, individual SWCNT can be classified as semiconducting (S-SWCNT) or metallic (M-SWCNT). In order to verify whether there would be differential toxicological effect of the two sorted SWCNTs, a library of SWCNTs was established with S-SWCNTs, M-SWCNTs, unsorted SWCNTs, or a remixed sample containing purified S-SWCNTs and M-SWCNTs in a 2:1 ratio. These materials were unique for the high purity levels (98.5% S-SWCNT and 98.8% M-SWCNT). The in vitro screening analysis indicated that in spite of their differences to induce ROS generation and oxidative stress, the toxicological outcome in the lung are similar for S- and M-SWCNTs. This indicated that the chirality or electrical property did not impact SWCNT toxicological profile independently in the lung, which could be of considerable importance to the safety assessment and incremental use of purified tubes by industry [20].

Another example of ECN is the 2-dimension (2D) carbonaceous nanomaterials, e.g. graphene and GO [14]. Although there are studies showing that they are able to induce toxicity in vitro and in vivo, the results are not conclusive and sometimes even contradictory. In addition, it is unclear about surface properties that are responsible for the toxicity, including reactive oxidation states and reactive surface groups on the planar surface. Among the reported effects of GO on the cell death mechanism, many studies have shown that GO could induce cell-death in a dose-dependent way on epithelial cells (BEAS-2B), macrophages (THP-1 and J774), and lung fibroblasts (HLF), etc. [19, 119]. However, these results were inconsistent and even contradictory in various mammalian cell models among different groups [119].Therefore, it is necessary to have a library of GOfrom the same batch with differential surface properties, such as pristine, reduced (rGO), and hydrated GO (hGO) etc, and to quantitatively determine their hydroxyl, carboxyl, epoxy, and carbon radical contentsbefore applying to in vitro and in vivo experimentation. It was found that hGO, which has the highest carbon radical density, exhibited the most cytotoxic effects because of reactive radical generation, cellular membrane lipid peroxidation and membrane lysis. This

could also be explained by the lack of cellular uptake and extensive adhesion of hGO on cell membrane. In contrast, pristine GO had lesser effects, while rGO showed minimal effects without lipid peroxidation, oxidative stress, and cytotoxicity. The in vivo results correlated well with the in vitro findings, in which hGO was more toxic than other materials in inducing acute lung inflammation, as evidenced by the highest level of lipid peroxidation in alveolar macrophages, cytokine production (LIX, MCP-1), and LDH release in bronchoalveolar lavage fluid. Pristine GO has less toxic effects and rGO shows little effects, similar to in vitro results. These findings showed that surface oxidation state and carbon radical content played major roles in GO toxicity. There are other studies which showed that the effects of additional physicochemical properties, such as planar surface area, number of layers and chemistry of functionalization etc., also play the role on their toxicity [120, 121]. One possible approach to reduce ECN cytotoxicity was surface functionalization, such as coating the ECNs with a tri-block copolymer (Pluronic F108), which decrease the cellular uptake, prevents the ECN-induced plasma or lysosomal membrane damage, and subsequent induction of inflammatory pathways [14], which could be a safer design approach to improve their stability and biocompatibility. The fifth example is the development of predictive toxicology paradigm for rare earth oxide nanomaterials (REO) [122]. The growing application of rare earth based materials, such as upconversion nanoparticles for biosensors, luminescence probes and Gadolinium (Gd)-based MRI contrast agents, increases the potential of human exposure [123–126]. The increasing biological use has generated the possibility for hazardous effects, not limited to the lung fibrosis in polishers and RE mining workers [127], but also the MRI agents could induce nephrogenic systemic fibrosis in patients [128]. Macrophage internalization of Gd could be noticed around the systemic sites of collagen deposition in those patients [129]. In addition, it is known that activated NLRP3 inflammasome is the major contributor for IL-1β secretion and pulmonary fibrosis [130]. While a number of studies showed that long aspect ratio ENMs, such as TiO_2 nanobelts, could promote pulmonary fibrosis through NLRP3 inflammasome activation [131]. However, it is not known whether REOs have the same pathway to trigger these side effects. Different from most of the transitional metals, the RE ions can bind to phosphate with high affinity. When dissolved under acidic environment, e.g., in lysosomes after cellular uptake, due to high binding affinity to phosphates, RE ions could deplete the phosphate groups from the lysosomal interior solutions and strip phosphates from lysosomal membrane, to form $REPO_4$. The precipitation of $REPO_4$ on particle surface leads to transformation of spherical REOs into urchin shaped structures. It is found that when these particles are taken up by macrophages, they localize inside lysosomes and they transformed to urchin shaped structures, which can damage the lysosomal membranes, resulting in cathepsin B release, NLRP3 inflammasome activation, IL-1β production and ultimately leading to pulmonary fibrosis. A series of analytical techniques were used to show this complex process. The dissolution tests were done by ICP-OES and TEM observation showed that all REO nanoparticles, except for CeO_2, underwent a complete morphological transformation in phagolysosomal simulated fluid (PSF, pH 4.5) and lysosomal compartments in the macrophages. The TEM analysis clearly showed that the light lanthanide nanoparticles (e.g., La_2O_3, Nd_2O_3, and Gd_2O_3) tend to form urchin shaped structures with needle-like protrusions, whereas the heavy lanthanide particles (e.g., Dy_2O_3, Er_2O_3, and Yb_2O_3) prefer to form mesh-like structures containing disordered nanowires. Similar morphological

changes were also observed by other studies [132–134]. Such morphological changes were not seen for the non-REO control particles, such as TiO_2. Both the XRD and EDS analysis confirm that the transformed urchin shaped structures are the $REPO_4$ precipitation due to complexation between RE(III) ions and phosphate from the membranes. The understanding of the mechanism of REO toxicity leads to safe design of lanthanide-based upconversion nanoparticles (UCNPs) [122]. Since it is known that lanthanide particles are dissolvable in acidic lysosomes, a series of phosphonate-based coatings to passivate particle surfaces through the complexation of phosphate groups with lanthanide elements. By using HTS strategy, it was verified that ethylenediamine tetra (methylelephosphonic acid) (EDTMP) could provide the most stable coating and protect lanthanide particles from dissolution under the acidic biological environment while maintaining their fluorescence properties. In addition, phosphonate coating decreased the pro-inflammatory effects of UCNPs in vitro and in vivo. Thus, EDTMP coating could be used as an effective safe-by-design method for UCNP biological applications, with the advantage of also preserving imaging properties.

4. Conclusion

In this review, we discussed the critical roles of analytical techniques in establishment of predictive toxicology for ENMs. The predictive toxicological approach involves building of compositional and combinatorial libraries, characterization of ENM physicochemical properties by analytical techniques, use of bioanalytical HTS methods to study the mechanism of toxicity induced by ENMs, and validation with in vivo studies. Robust analytical techniques and assays for characterization of nanomaterials physicochemical properties abiotically, in vitro and in vivo are especially important to link to their properties to toxicity and build the structure activity relationships. Ultimately, the creative use of optimal techniques, and the toxicity screening approach we advocate, will provide valuable guidance for designing safer nanomaterials for their future applications.

Acknowledgments

Research reported in this publication was supported by the National Institute of Environmental Health Sciences at the National Institutes of Health, under Award Nos. U01ES027237 and RO1ES022698. Leveraged support for characterization equipment used in this study was provided by the National Science Foundation and the Environmental Protection Agency under Award No. DBI-1266377.

References

1. Liu Y, Zhou G, Liu K, Cui Y. Design of Complex Nanomaterials for Energy Storage: Past Success and Future Opportunity. Acc Chem Res. 2017; 50(12):2895–905. [PubMed: 29206446]
2. Park SJ, Ok JG, Park HJ, Lee K-T, Lee JH, Kim JD, et al. Modulation of the effective density and refractive index of carbon nanotube forests via nanoimprint lithography. Carbon. 2018; 129:8–14.
3. Abdalla AM, Hossain S, Azad AT, Petra PMI, Begum F, Eriksson SG, et al. Nanomaterials for solid oxide fuel cells: A review. Renewable Sustainable Energy Rev. 2018; 82:353–68.
4. Chen X, Mao SS. Titanium Dioxide Nanomaterials: Synthesis, Properties, Modifications, and Applications. Chem Rev. 2007; 107(7):2891–959. [PubMed: 17590053]
5. Jain PK, Huang X, El-Sayed IH, El-Sayed MA. Noble Metals on the Nanoscale: Optical and Photothermal Properties and Some Applications in Imaging, Sensing, Biology, and Medicine. Acc Chem Res. 2008; 41(12):1578–86. [PubMed: 18447366]

6. Nel A, Xia T, Mädler L, Li N. Toxic Potential of Materials at the Nanolevel. Science. 2006; 311(5761):622–7. [PubMed: 16456071]
7. Meng H, Xia T, George S, Nel AE. A Predictive Toxicological Paradigm for the Safety Assessment of Nanomaterials. ACS Nano. 2009; 3(7):1620–7. [PubMed: 21452863]
8. Nel A, Xia T, Meng H, Wang X, Lin S, Ji Z, et al. Nanomaterial toxicity testing in the 21st century: use of a predictive toxicological approach and high-throughput screening. Acc Chem Res. 2013; 46(3):607–21. [PubMed: 22676423]
9. Nel AE, Mädler L, Velegol D, Xia T, Hoek EMV, Somasundaran P, et al. Understanding biophysicochemical interactions at the nano–bio interface. Nat Mater. 2009; 8:543. [PubMed: 19525947]
10. Chen P-C, Liu X, Hedrick JL, Xie Z, Wang S, Lin Q-Y, et al. Polyelemental nanoparticle libraries. Science. 2016; 352(6293):1565–9. [PubMed: 27339985]
11. George S, Pokhrel S, Ji Z, Henderson BL, Xia T, Li L, et al. Role of Fe Doping in Tuning the Band Gap of TiO_2 for the Photo-Oxidation-Induced Cytotoxicity Paradigm. J Am Chem Soc. 2011; 133(29):11270–8. [PubMed: 21678906]
12. Ji Z, Wang X, Zhang H, Lin S, Meng H, Sun B, et al. Designed Synthesis of CeO_2 Nanorods and Nanowires for Studying Toxicological Effects of High Aspect Ratio Nanomaterials. ACS Nano. 2012; 6(6):5366–80. [PubMed: 22564147]
13. Meng H, Yang S, Li Z, Xia T, Chen J, Ji Z, et al. Aspect Ratio Determines the Quantity of Mesoporous Silica Nanoparticle Uptake by a Small GTPase-Dependent Macropinocytosis Mechanism. ACS Nano. 2011; 5(6):4434–47. [PubMed: 21563770]
14. Wang X, Xia T, Duch MC, Ji Z, Zhang H, Li R, et al. Pluronic F108 Coating Decreases the Lung Fibrosis Potential of Multiwall Carbon Nanotubes by Reducing Lysosomal Injury. Nano Lett. 2012; 12(6):3050–61. [PubMed: 22546002]
15. Xia T, Kovochich M, Liong M, Zink JI, Nel AE. Cationic Polystyrene Nanosphere Toxicity Depends on Cell-Specific Endocytic and Mitochondrial Injury Pathways. ACS Nano. 2008; 2(1): 85–96. [PubMed: 19206551]
16. Zhang H, Xia T, Meng H, Xue M, George S, Ji Z, et al. Differential Expression of Syndecan-1 Mediates Cationic Nanoparticle Toxicity in Undifferentiated versus Differentiated Normal Human Bronchial Epithelial Cells. ACS Nano. 2011; 5(4):2756–69. [PubMed: 21366263]
17. Lin S, Wang X, Ji Z, Chang CH, Dong Y, Meng H, et al. Aspect Ratio Plays a Role in the Hazard Potential of CeO_2 Nanoparticles in Mouse Lung and Zebrafish Gastrointestinal Tract. ACS Nano. 2014; 8(5):4450–64. [PubMed: 24720650]
18. Xia T, Zhao Y, Sager T, George S, Pokhrel S, Li N, et al. Decreased Dissolution of ZnO by Iron Doping Yields Nanoparticles with Reduced Toxicity in the Rodent Lung and Zebrafish Embryos. ACS Nano. 2011; 5(2):1223–35. [PubMed: 21250651]
19. Li R, Guiney LM, Chang CH, Mansukhani ND, Ji Z, Wang X, et al. Surface Oxidation of Graphene Oxide Determines Membrane Damage, Lipid Peroxidation, and Cytotoxicity in Macrophages in a Pulmonary Toxicity Model. ACS Nano. 2018; 12(2):1390–402. [PubMed: 29328670]
20. Wang X, Mansukhani ND, Guiney LM, Lee J-H, Li R, Sun B, et al. Toxicological Profiling of Highly Purified Metallic and Semiconducting Single-Walled Carbon Nanotubes in the Rodent Lung and E. coli. ACS Nano. 2016; 10(6):6008–19. [PubMed: 27159184]
21. Li R, Wang X, Ji Z, Sun B, Zhang H, Chang CH, et al. Surface Charge and Cellular Processing of Covalently Functionalized Multiwall Carbon Nanotubes Determine Pulmonary Toxicity. ACS Nano. 2013; 7(3):2352–68. [PubMed: 23414138]
22. Hall JB, Dobrovolskaia MA, Patri AK, McNeil SE. Characterization of nanoparticles for therapeutics. Nanomedicine. 2007; 2(6):789–803. [PubMed: 18095846]
23. Farokhzad OC, Langer R. Nanomedicine: Developing smarter therapeutic and diagnostic modalities. Adv Drug Deliv Rev. 2006; 58(14):1456–9. [PubMed: 17070960]
24. Ji Z. Use of compositional and combinatorial nanomaterial libraries for biological studies. Science Bulletin. 2016; 61(10):755–71.

25. Sun B, Li R, Wang X, Xia T. Predictive toxicological paradigm and high throughput approach for toxicity screening of engineered nanomaterials. International Journal of Biomedical Nanoscience and Nanotechnology. 2013; 3(1–2):4–18.
26. Bibette J. Gaining confidence in high-throughput screening. Proceedings of the National Academy of Sciences. 2012; 109(3):649–50.
27. Malo N, Hanley JA, Cerquozzi S, Pelletier J, Nadon R. Statistical practice in high-throughput screening data analysis. Nat Biotechnol. 2006; 24:167. [PubMed: 16465162]
28. Inglese J, Auld DS, Jadhav A, Johnson RL, Simeonov A, Yasgar A, et al. Quantitative high-throughput screening: A titration-based approach that efficiently identifies biological activities in large chemical libraries. Proceedings of the National Academy of Sciences. 2006; 103(31):11473–8.
29. Miller OJ, Harrak AE, Mangeat T, Baret J-C, Frenz L, Debs BE, et al. High-resolution dose–response screening using droplet-based microfluidics. Proceedings of the National Academy of Sciences. 2012; 109(2):378–83.
30. Pal AK, Watson CY, Pirela SV, Singh D, Chalbot M-CG, Kavouras I, et al. Linking Exposures of Particles Released From Nano-Enabled Products to Toxicology: An Integrated Methodology for Particle Sampling, Extraction, Dispersion, and Dosing. Toxicol Sci. 2015; 146(2):321–33. [PubMed: 25997654]
31. DeLoid GM, Cohen JM, Pyrgiotakis G, Pirela SV, Pal A, Liu J, et al. Advanced computational modeling for in vitro nanomaterial dosimetry. Particle and Fibre Toxicology. 2015; 12(1):32. [PubMed: 26497802]
32. Cohen JM, Teeguarden JG, Demokritou P. An integrated approach for the in vitro dosimetry of engineered nanomaterials. Particle and Fibre Toxicology. 2014; 11(1):20. [PubMed: 24885440]
33. Pirela SV, Miousse IR, Lu X, Castranova V, Thomas T, Qian Y, et al. Effects of Laser Printer–Emitted Engineered Nanoparticles on Cytotoxicity, Chemokine Expression, Reactive Oxygen Species, DNA Methylation, and DNA Damage: A Comprehensive in Vitro Analysis in Human Small Airway Epithelial Cells, Macrophages, and Lymphoblasts. Environ Health Perspect. 2016; 124(2):210–9. [PubMed: 26080392]
34. Hinderliter PM, Minard KR, Orr G, Chrisler WB, Thrall BD, Pounds JG, et al. ISDD: A computational model of particle sedimentation, diffusion and target cell dosimetry for in vitro toxicity studies. Particle and Fibre Toxicology. 2010; 7(1):36. [PubMed: 21118529]
35. DeLoid G, Cohen JM, Darrah T, Derk R, Rojanasakul L, Pyrgiotakis G, et al. Estimating the effective density of engineered nanomaterials for in vitro dosimetry. Nature communications. 2014; 5:3514.
36. DeLoid GM, Cohen JM, Pyrgiotakis G, Demokritou P. Preparation, characterization, and in vitro dosimetry of dispersed, engineered nanomaterials. Nat Protoc. 2017; 12:355. [PubMed: 28102836]
37. Lin W, Huang Y-w, Zhou X-D, Ma Y. In vitro toxicity of silica nanoparticles in human lung cancer cells. Toxicol Appl Pharmacol. 2006; 217(3):252–9. [PubMed: 17112558]
38. George S, Pokhrel S, Xia T, Gilbert B, Ji Z, Schowalter M, et al. Use of a Rapid Cytotoxicity Screening Approach To Engineer a Safer Zinc Oxide Nanoparticle through Iron Doping. ACS Nano. 2010; 4(1):15–29. [PubMed: 20043640]
39. Zhang H, Ji Z, Xia T, Meng H, Low-Kam C, Liu R, et al. Use of Metal Oxide Nanoparticle Band Gap To Develop a Predictive Paradigm for Oxidative Stress and Acute Pulmonary Inflammation. ACS Nano. 2012; 6(5):4349–68. [PubMed: 22502734]
40. Yue H, Wei W, Yue Z, Wang B, Luo N, Gao Y, et al. The role of the lateral dimension of graphene oxide in the regulation of cellular responses. Biomaterials. 2012; 33(16):4013–21. [PubMed: 22381473]
41. Sun B, Wang X, Ji Z, Wang M, Liao YP, Chang CH, et al. NADPH Oxidase-Dependent NLRP3 Inflammasome Activation and its Important Role in Lung Fibrosis by Multiwalled Carbon Nanotubes. Small. 2015; 11(17):2087–97. [PubMed: 25581126]
42. Reifarth M, Hoeppener S, Schubert US. Uptake and Intracellular Fate of Engineered Nanoparticles in Mammalian Cells: Capabilities and Limitations of Transmission Electron Microscopy—Polymer-Based Nanoparticles. Adv Mater. 2018; 30(9):1703704.

43. Kitani H, Sakuma C, Takenouchi T, Sato M, Yoshioka M, Yamanaka N. Establishment of c-myc-immortalized Kupffer cell line from a C57BL/6 mouse strain. Results in Immunology. 2014; 4:68–74. [PubMed: 25379377]
44. Bilzer M, Roggel F, Gerbes AL. Role of Kupffer cells in host defense and liver disease. Liver International. 2006; 26(10):1175–86. [PubMed: 17105582]
45. Godoy P, Hewitt NJ, Albrecht U, Andersen ME, Ansari N, Bhattacharya S, et al. Recent advances in 2D and 3D in vitro systems using primary hepatocytes, alternative hepatocyte sources and non-parenchymal liver cells and their use in investigating mechanisms of hepatotoxicity, cell signaling and ADME. Arch Toxicol. 2013; 87(8):1315–530. [PubMed: 23974980]
46. Wang X, Ji Z, Chang CH, Zhang H, Wang M, Liao YP, et al. Use of Coated Silver Nanoparticles to Understand the Relationship of Particle Dissolution and Bioavailability to Cell and Lung Toxicological Potential. Small. 2014; 10(2):385–98. [PubMed: 24039004]
47. Li N, Hao M, Phalen RF, Hinds WC, Nel AE. Particulate air pollutants and asthma: A paradigm for the role of oxidative stress in PM-induced adverse health effects. Clin Immunol. 2003; 109(3): 250–65. [PubMed: 14697739]
48. Poland CA, Duffin R, Kinloch I, Maynard A, Wallace WAH, Seaton A, et al. Carbon nanotubes introduced into the abdominal cavity of mice show asbestos-like pathogenicity in a pilot study. Nat Nanotechnol. 2008; 3:423. [PubMed: 18654567]
49. Xia T, Kovochich M, Liong M, Mädler L, Gilbert B, Shi H, et al. Comparison of the Mechanism of Toxicity of Zinc Oxide and Cerium Oxide Nanoparticles Based on Dissolution and Oxidative Stress Properties. ACS Nano. 2008; 2(10):2121–34. [PubMed: 19206459]
50. Sun B, Pokhrel S, Dunphy DR, Zhang H, Ji Z, Wang X, et al. Reduction of Acute Inflammatory Effects of Fumed Silica Nanoparticles in the Lung by Adjusting Silanol Display through Calcination and Metal Doping. ACS Nano. 2015; 9(9):9357–72. [PubMed: 26200133]
51. Pietropaoli AP, Frampton MW, Hyde RW, Morrow PE, Oberdörster G, Cox C, et al. Pulmonary Function, Diffusing Capacity, and Inflammation in Healthy and Asthmatic Subjects Exposed to Ultrafine Particles. Inhal Toxicol. 2004; 16(sup1):59–72. [PubMed: 15204794]
52. Kermanizadeh A, Lhr M, Roursgaard M, Messner S, Gunness P, Kelm JM, et al. Hepatic toxicology following single and multiple exposure of engineered nanomaterials utilising a novel primary human 3D liver microtissue model. Particle and Fibre Toxicology. 2014; 11(1):56. [PubMed: 25326698]
53. Moyano Daniel F, Liu Y, Ayaz F, Hou S, Puangploy P, Duncan B, et al. Immunomodulatory Effects of Coated Gold Nanoparticles in LPS-Stimulated In Vitro and In Vivo Murine Model Systems. Chem. 2016; 1(2):320–7. [PubMed: 28255579]
54. Dellinger AL, Cunin P, Lee D, Kung AL, Brooks DB, Zhou Z, et al. Inhibition of Inflammatory Arthritis Using Fullerene Nanomaterials. PLOS ONE. 2015; 10(4):e0126290. [PubMed: 25879437]
55. Li R, Ji Z, Qin H, Kang X, Sun B, Wang M, et al. Interference in Autophagosome Fusion by Rare Earth Nanoparticles Disrupts Autophagic Flux and Regulation of an Interleukin-1β Producing Inflammasome. ACS Nano. 2014; 8(10):10280–92. [PubMed: 25251502]
56. Li R, Ji Z, Chang CH, Dunphy DR, Cai X, Meng H, et al. Surface Interactions with Compartmentalized Cellular Phosphates Explain Rare Earth Oxide Nanoparticle Hazard and Provide Opportunities for Safer Design. ACS Nano. 2014; 8(2):1771–83. [PubMed: 24417322]
57. Herd HL, Malugin A, Ghandehari H. Silica nanoconstruct cellular toleration threshold in vitro. J Controlled Release. 2011; 153(1):40–8.
58. Riss TL, Moravec RA. Use of Multiple Assay Endpoints to Investigate the Effects of Incubation Time, Dose of Toxin, and Plating Density in Cell-Based Cytotoxicity Assays. ASSAY and Drug Development Technologies. 2004; 2(1):51–62. [PubMed: 15090210]
59. Mukhopadhyay P, Rajesh M, Yoshihiro K, Haskó G, Pacher P. Simple quantitative detection of mitochondrial superoxide production in live cells. Biochem Biophys Res Commun. 2007; 358(1): 203–8. [PubMed: 17475217]
60. Hirota JA, Hirota SA, Warner SM, Stefanowicz D, Shaheen F, Beck PL, et al. The airway epithelium nucleotide-binding domain and leucine-rich repeat protein 3 inflammasome is activated

by urban particulate matter. J Allergy Clin Immun. 2012; 129(4):1116–25.e6. [PubMed: 22227418]

61. Li R, Mansukhani ND, Guiney LM, Ji Z, Zhao Y, Chang CH, et al. Identification and Optimization of Carbon Radicals on Hydrated Graphene Oxide for Ubiquitous Antibacterial Coatings. ACS Nano. 2016; 10(12):10966–80. [PubMed: 28024366]
62. Dunbar SA, Vander Zee CA, Oliver KG, Karem KL, Jacobson JW. Quantitative, multiplexed detection of bacterial pathogens: DNA and protein applications of the Luminex LabMAP™ system. J Microbiol Methods. 2003; 53(2):245–52. [PubMed: 12654495]
63. Dunbar SA. Applications of Luminex® xMAP™ technology for rapid, high-throughput multiplexed nucleic acid detection. Clin Chim Acta. 2006; 363(1):71–82. [PubMed: 16102740]
64. Hoare R, Thompson KD, Herath T, Collet B, Bron JE, Adams A. Development, Characterisation and Application of Monoclonal Antibodies for the Detection and Quantification of Infectious Salmon Anaemia Virus in Plasma Samples Using Luminex Bead Array Technology. PLOS ONE. 2016; 11(7):e0159155. [PubMed: 27434377]
65. Chuang C-K, Lin H-Y, Wang T-J, Huang S-F, Lin SP. Bio-Plex immunoassay measuring the quantity of lysosomal *N*-acetylgalactosamine-6-sulfatase protein in dried blood spots for the screening of mucopolysaccharidosis IVA in newborn: a pilot study. BMJ Open. 2017; 7(7)
66. Ling MM, Ricks C, Lea P. Multiplexing molecular diagnostics and immunoassays using emerging microarray technologies. Expert Review of Molecular Diagnostics. 2007; 7(1):87–98. [PubMed: 17187487]
67. Ullman EF, Kirakossian H, Switchenko AC, Ishkanian J, Ericson M, Wartchow CA, et al. Luminescent oxygen channeling assay (LOCI): sensitive, broadly applicable homogeneous immunoassay method. Clin Chem. 1996; 42(9):1518–26. [PubMed: 8787723]
68. Beaudet L, Rodriguez-Suarez R, Venne M-H, Caron M, Bédard J, Brechler V, et al. AlphaLISA immunoassays: the no-wash alternative to ELISAs for research and drug discovery. Nat Methods. 2008; 5
69. Poulsen F, Jensen KB. A Luminescent Oxygen Channeling Immunoassay for the Determination of Insulin in Human Plasma. J Biomol Screening. 2007; 12(2):240–7.
70. Gaudin R, Barteneva NS. Sorting of small infectious virus particles by flow virometry reveals distinct infectivity profiles. Nature communications. 2015; 6:6022.
71. Breton G, Lee J, Liu K, Nussenzweig MC. Defining human dendritic cell progenitors by multiparametric flow cytometry. Nat Protoc. 2015; 10:1407. [PubMed: 26292072]
72. Porichis F, Hart MG, Griesbeck M, Everett HL, Hassan M, Baxter AE, et al. High-throughput detection of miRNAs and gene-specific mRNA at the single-cell level by flow cytometry. Nature communications. 2014; 5:5641.
73. Chattopadhyay PK, Gierahn TM, Roederer M, Love JC. Single-cell technologies for monitoring immune systems. Nat Immunol. 2014; 15:128. [PubMed: 24448570]
74. Luo N, Weber JK, Wang S, Luan B, Yue H, Xi X, et al. PEGylated graphene oxide elicits strong immunological responses despite surface passivation. Nature communications. 2017; 8:14537.
75. Keustermans GCE, Hoeks SBE, Meerding Jenny M, Prakken BJ, de Jager W. Cytokine assays: An assessment of the preparation and treatment of blood and tissue samples. Methods. 2013; 61(1): 10–7. [PubMed: 23603216]
76. Chithrani BD, Ghazani AA, Chan WCW. Determining the Size and Shape Dependence of Gold Nanoparticle Uptake into Mammalian Cells. Nano Lett. 2006; 6(4):662–8. [PubMed: 16608261]
77. Wilson MR, Lightbody JH, Donaldson K, Sales J, Stone V. Interactions between Ultrafine Particles and Transition Metals in Vivo and in Vitro. Toxicol Appl Pharmacol. 2002; 184(3):172–9. [PubMed: 12460745]
78. Lorenz MR, Holzapfel V, Musyanovych A, Nothelfer K, Walther P, Frank H, et al. Uptake of functionalized, fluorescent-labeled polymeric particles in different cell lines and stem cells. Biomaterials. 2006; 27(14):2820–8. [PubMed: 16430958]
79. Li N, Xia T, Nel AE. The role of oxidative stress in ambient particulate matter-induced lung diseases and its implications in the toxicity of engineered nanoparticles. Free Radical Biol Med. 2008; 44(9):1689–99. [PubMed: 18313407]

80. Xia T, Kovochich M, Brant J, Hotze M, Sempf J, Oberley T, et al. Comparison of the Abilities of Ambient and Manufactured Nanoparticles To Induce Cellular Toxicity According to an Oxidative Stress Paradigm. Nano Lett. 2006; 6(8):1794–807. [PubMed: 16895376]
81. Xia T, Li N, Nel AE. Potential Health Impact of Nanoparticles. Annu Rev Publ Health. 2009; 30(1):137–50.
82. Abraham VC, Taylor DL, Haskins JR. High content screening applied to large-scale cell biology. Trends Biotechnol. 2004; 22(1):15–22. [PubMed: 14690618]
83. Abraham VC, Towne DL, Waring JF, Warrior U, Burns DJ. Application of a High-Content Multiparameter Cytotoxicity Assay to Prioritize Compounds Based on Toxicity Potential in Humans. J Biomol Screening. 2008; 13(6):527–37.
84. Rushton EK, Jiang J, Leonard SS, Eberly S, Castranova V, Biswas P, et al. Concept of Assessing Nanoparticle Hazards Considering Nanoparticle Dosemetric and Chemical/Biological Response Metrics. Journal of Toxicology and Environmental Health, Part A. 2010; 73(5–6):445–61. [PubMed: 20155585]
85. Cho WS, Duffin R, Poland CA, Howie SE, MacNee W, Bradley M, et al. Metal oxide nanoparticles induce unique inflammatory footprints in the lung: important implications for nanoparticle testing. Environ Health Perspect. 2010; 118(12):1699–706. [PubMed: 20729176]
86. Lu S, Duffin R, Poland C, Daly P, Murphy F, Drost E, et al. Efficacy of simple short-term in vitro assays for predicting the potential of metal oxide nanoparticles to cause pulmonary inflammation. Environ Health Perspect. 2009; 117(2):241–7. [PubMed: 19270794]
87. Portier J, Campet G, Poquet A, Marcel C, Subramanian MA. Degenerate semiconductors in the light of electronegativity and chemical hardness. Int J Inorg Mater. 2001; 3(7):1039–43.
88. Migdal C, Rahal R, Rubod A, Callejon S, Colomb E, Atrux-Tallau N, et al. Internalisation of hybrid titanium dioxide/para-amino benzoic acid nanoparticles in human dendritic cells did not induce toxicity and changes in their functions. Toxicol Lett. 2010; 199(1):34–42. [PubMed: 20699112]
89. Zhang H, Dunphy DR, Jiang X, Meng H, Sun B, Tarn D, et al. Processing Pathway Dependence of Amorphous Silica Nanoparticle Toxicity: Colloidal vs Pyrolytic. J Am Chem Soc. 2012; 134(38): 15790–804. [PubMed: 22924492]
90. Sun B, Wang X, Liao Y-P, Ji Z, Chang CH, Pokhrel S, et al. Repetitive Dosing of Fumed Silica Leads to Profibrogenic Effects through Unique Structure–Activity Relationships and Biopersistence in the Lung. ACS Nano. 2016; 10(8):8054–66. [PubMed: 27483033]
91. Ghiazza M, Polimeni M, Fenoglio I, Gazzano E, Ghigo D, Fubini B. Does Vitreous Silica Contradict the Toxicity of the Crystalline Silica Paradigm? Chem Res Toxicol. 2010; 23(3):620–9. [PubMed: 20085295]
92. Trofymluk O, Levchenko AA, Tolbert SH, Navrotsky A. Energetics of Mesoporous Silica: Investigation into Pore Size and Symmetry. Chem Mater. 2005; 17(14):3772–83.
93. Fubini B, Hubbard A. Reactive oxygen species (ROS) and reactive nitrogen species (RNS) generation by silica in inflammation and fibrosis. Free Radic Biol Med. 2003; 34(12):1507–16. [PubMed: 12788471]
94. Castranova V, Vallyathan V. Silicosis and coal workers' pneumoconiosis. Environ Health Perspect. 2000; 108(Suppl 4):675–84.
95. Fubini B. Surface Chemistery and Quartz Hazard. The Annals of Occupational Hygiene. 1998; 42(8):521–30. [PubMed: 9838865]
96. Lin Y-S, Haynes CL. Impacts of Mesoporous Silica Nanoparticle Size, Pore Ordering, and Pore Integrity on Hemolytic Activity. J Am Chem Soc. 2010; 132(13):4834–42. [PubMed: 20230032]
97. Maurer-Jones MA, Lin Y-S, Haynes CL. Functional Assessment of Metal Oxide Nanoparticle Toxicity in Immune Cells. ACS Nano. 2010; 4(6):3363–73. [PubMed: 20481555]
98. Qianjun H, Zhiwen Z, Yu G, Jianlin S, Yaping L. Intracellular Localization and Cytotoxicity of Spherical Mesoporous Silica Nano- and Microparticles. Small. 2009; 5(23):2722–9. [PubMed: 19780070]
99. Thomassen LCJ, Aerts A, Rabolli V, Lison D, Gonzalez L, Kirsch-Volders M, et al. Synthesis and Characterization of Stable Monodisperse Silica Nanoparticle Sols for in Vitro Cytotoxicity Testing. Langmuir. 2010; 26(1):328–35. [PubMed: 19697952]

100. Slowing II, Wu CW, Vivero-Escoto JL, Lin VS-Y. Mesoporous Silica Nanoparticles for Reducing Hemolytic Activity Towards Mammalian Red Blood Cells. Small. 2009; 5(1):57–62. [PubMed: 19051185]
101. Yu T, Malugin A, Ghandehari H. Impact of Silica Nanoparticle Design on Cellular Toxicity and Hemolytic Activity. ACS Nano. 2011; 5(7):5717–28. [PubMed: 21630682]
102. Fadeel B, Garcia-Bennett AE. Better safe than sorry: Understanding the toxicological properties of inorganic nanoparticles manufactured for biomedical applications. Adv Drug Deliv Rev. 2010; 62(3):362–74. [PubMed: 19900497]
103. Yan W, Bernd N. Environmental risk assessment of engineered nano-SiO_2, nano iron oxides, nano-CeO_2, nano-Al_2O_3, and quantum dots. Environ Toxicol Chem. 2018; 37(5):1387–95. [PubMed: 29315795]
104. Setyawati MI, Tay CY, Leong DT. Nanotoxicity: Mechanistic Investigation of the Biological Effects of SiO_2, TiO_2, and ZnO Nanoparticles on Intestinal Cells (Small 28/2015). Small. 2015; 11(28):3458–68. [PubMed: 25902938]
105. Angela I, Tiina T, Meeri V, Heiki V, Aleksandr K, Mariliis S, et al. Toxicity of 11 Metal Oxide Nanoparticles to Three Mammalian Cell Types In Vitro. Curr Top Med Chem. 2015; 15(18): 1914–29. [PubMed: 25961521]
106. Wang X, Xia T, Ntim SA, Ji Z, George S, Meng H, et al. Quantitative Techniques for Assessing and Controlling the Dispersion and Biological Effects of Multiwalled Carbon Nanotubes in Mammalian Tissue Culture Cells. ACS Nano. 2010; 4(12):7241–52. [PubMed: 21067152]
107. Wang X, Xia T, Addo Ntim S, Ji Z, Lin S, Meng H, et al. Dispersal State of Multiwalled Carbon Nanotubes Elicits Profibrogenic Cellular Responses That Correlate with Fibrogenesis Biomarkers and Fibrosis in the Murine Lung. ACS Nano. 2011; 5(12):9772–87. [PubMed: 22047207]
108. Wang X, Duch MC, Mansukhani N, Ji Z, Liao Y-P, Wang M, et al. Use of a Pro-Fibrogenic Mechanism-Based Predictive Toxicological Approach for Tiered Testing and Decision Analysis of Carbonaceous Nanomaterials. ACS Nano. 2015; 9(3):3032–43. [PubMed: 25646681]
109. Wang X, Liao YP, Telesca D, Chang CH, Xia T, Nel AE. The Genetic Heterogeneity among Different Mouse Strains Impacts the Lung Injury Potential of Multiwalled Carbon Nanotubes. Small. 2017; 13(33):1700776.
110. Wu H-C, Chang X, Liu L, Zhao F, Zhao Y. Chemistry of carbon nanotubes in biomedical applications. J Mater Chem. 2010; 20(6):1036–52.
111. Liu M, Chen B, Xue Y, Huang J, Zhang L, Huang S, et al. Polyamidoamine-Grafted Multiwalled Carbon Nanotubes for Gene Delivery: Synthesis, Transfection and Intracellular Trafficking. Bioconjugate Chem. 2011; 22(11):2237–43.
112. Varkouhi AK, Foillard S, Lammers T, Schiffelers RM, Doris E, Hennink WE, et al. SiRNA delivery with functionalized carbon nanotubes. Int J Pharm. 2011; 416(2):419–25. [PubMed: 21320582]
113. Rahimpour A, Jahanshahi M, Khalili S, Mollahosseini A, Zirepour A, Rajaeian B. Novel functionalized carbon nanotubes for improving the surface properties and performance of polyethersulfone (PES) membrane. Desalination. 2012; 286:99–107.
114. Foillard S, Zuber G, Doris E. Polyethylenimine–carbon nanotube nanohybrids for siRNA-mediated gene silencing at cellular level. Nanoscale. 2011; 3(4):1461–4. [PubMed: 21301705]
115. Hong SY, Tobias G, Al-Jamal KT, Ballesteros B, Ali-Boucetta H, Lozano-Perez S, et al. Filled and glycosylated carbon nanotubes for in vivo radioemitter localization and imaging. Nat Mater. 2010; 9:485. [PubMed: 20473287]
116. Wei W, Sébastien W, Giorgia P, Monica B, Cédric K, Jean-Paul B, et al. Targeted Delivery of Amphotericin B to Cells by Using Functionalized Carbon Nanotubes. Angewandte Chemie. 2005; 117(39):6516–20.
117. Xiang W, Jae-Hyeok L, Ruibin L, Yu-Pei L, Joohoon K, Hyun CC, et al. Toxicological Profiling of Highly Purified Single-Walled Carbon Nanotubes with Different Lengths in the Rodent Lung and Escherichia Coli. Small. 2018; 14:1703915.
118. Roda E, Coccini T, Barni S, Manzo L. Comparative pulmonary toxicity assessment of pristine and functionalized multi-walled carbon nanotubes intratracheally instilled in rats. Toxicol Lett. 2010; 196:S277.

119. Zhang B, Wei P, Zhou Z, Wei T. Interactions of graphene with mammalian cells: Molecular mechanisms and biomedical insights. Adv Drug Deliv Rev. 2016; 105:145–62. [PubMed: 27569910]
120. Minkyu K, G CW, Woong KJ, J GM, Katharina R, D OB. Hydrogels: Artificially Engineered Protein Hydrogels Adapted from the Nucleoporin Nsp1 for Selective Biomolecular Transport (Adv. Mater. 28/2015). Adv Mater. 2015; 27(28):4244.
121. Xiaoming L, Wei L, Lianwen S, E AK, Bo Y, Yubo F, et al. Effects of physicochemical properties of nanomaterials on their toxicity. Journal of Biomedical Materials Research Part A. 2015; 103(7):2499–507. [PubMed: 25530348]
122. Li R, Ji Z, Dong J, Chang CH, Wang X, Sun B, et al. Enhancing the Imaging and Biosafety of Upconversion Nanoparticles through Phosphonate Coating. ACS Nano. 2015; 9(3):3293–306. [PubMed: 25727446]
123. Ahrén M, Selegård L, Klasson A, Söderlind F, Abrikossova N, Skoglund C, et al. Synthesis and Characterization of PEGylated Gd_2O_3 Nanoparticles for MRI Contrast Enhancement. Langmuir. 2010; 26(8):5753–62. [PubMed: 20334417]
124. Bouzigues C, Gacoin T, Alexandrou A. Biological Applications of Rare-Earth Based Nanoparticles. ACS Nano. 2011; 5(11):8488–505. [PubMed: 21981700]
125. Hu CG, Liu H, Dong WT, Zhang YY, Bao G, Lao CS, Wang ZL. $La(OH)_3$ and La_2O_3 Nanobelts—Synthesis and Physical Properties. Adv Mater. 2007; 19(3):470–4.
126. Louis C, Bazzi R, Marquette CA, Bridot J-L, Roux S, Ledoux G, et al. Nanosized Hybrid Particles with Double Luminescence for Biological Labeling. Chem Mater. 2005; 17(7):1673–82.
127. Vocaturo G, Colombo F, Zanoni M, Rodi F, Sabbioni E, Pietra R. Human Exposure to Heavy Metals: Rare Earth Pneumoconiosis in Occupational Workers. Chest. 1983; 83(5):780–3. [PubMed: 6839821]
128. Marckmann P, Skov L, Rossen K, Dupont A, Damholt MB, Heaf JG, et al. Nephrogenic Systemic Fibrosis: Suspected Causative Role of Gadodiamide Used for Contrast-Enhanced Magnetic Resonance Imaging. J Am Soc Nephrol. 2006; 17(9):2359–62. [PubMed: 16885403]
129. Schmidt-Lauber C, Bossaller L, Abujudeh HH, Vladimer GI, Christ A, Fitzgerald KA, et al. Gadolinium-based compounds induce NLRP3-dependent IL-1β production and peritoneal inflammation. Ann Rheum Dis. 2015; 74(11):2062–9. [PubMed: 24914072]
130. Cassel SL, Eisenbarth SC, Iyer SS, Sadler JJ, Colegio OR, Tephly LA, et al. The Nalp3 inflammasome is essential for the development of silicosis. Proceedings of the National Academy of Sciences. 2008; 105(26):9035–40.
131. Hamilton RF, Wu N, Porter D, Buford M, Wolfarth M, Holian A. Particle length-dependent titanium dioxide nanomaterials toxicity and bioactivity. Particle and Fibre Toxicology. 2009; 6(1):35. [PubMed: 20043844]
132. Ma Y, He X, Zhang P, Zhang Z, Guo Z, Tai R, et al. Phytotoxicity and biotransformation of La_2O_3 nanoparticles in a terrestrial plant cucumber (Cucumis sativus). Nanotoxicology. 2011; 5(4):743–53. [PubMed: 21261455]
133. Le Y, Yang L, Na M, Shu-Hong Y, Long-Ping W. Rare Earth Oxide Nanocrystals Induce Autophagy in HeLa Cells. Small. 2009; 5(24):2784–7. [PubMed: 19885892]
134. Sisler JD, Li R, McKinney W, Mercer RR, Ji Z, Xia T, et al. Differential pulmonary effects of CoO and La_2O_3 metal oxide nanoparticle responses during aerosolized inhalation in mice. Particle and Fibre Toxicology. 2016; 13(1):42. [PubMed: 27527840]

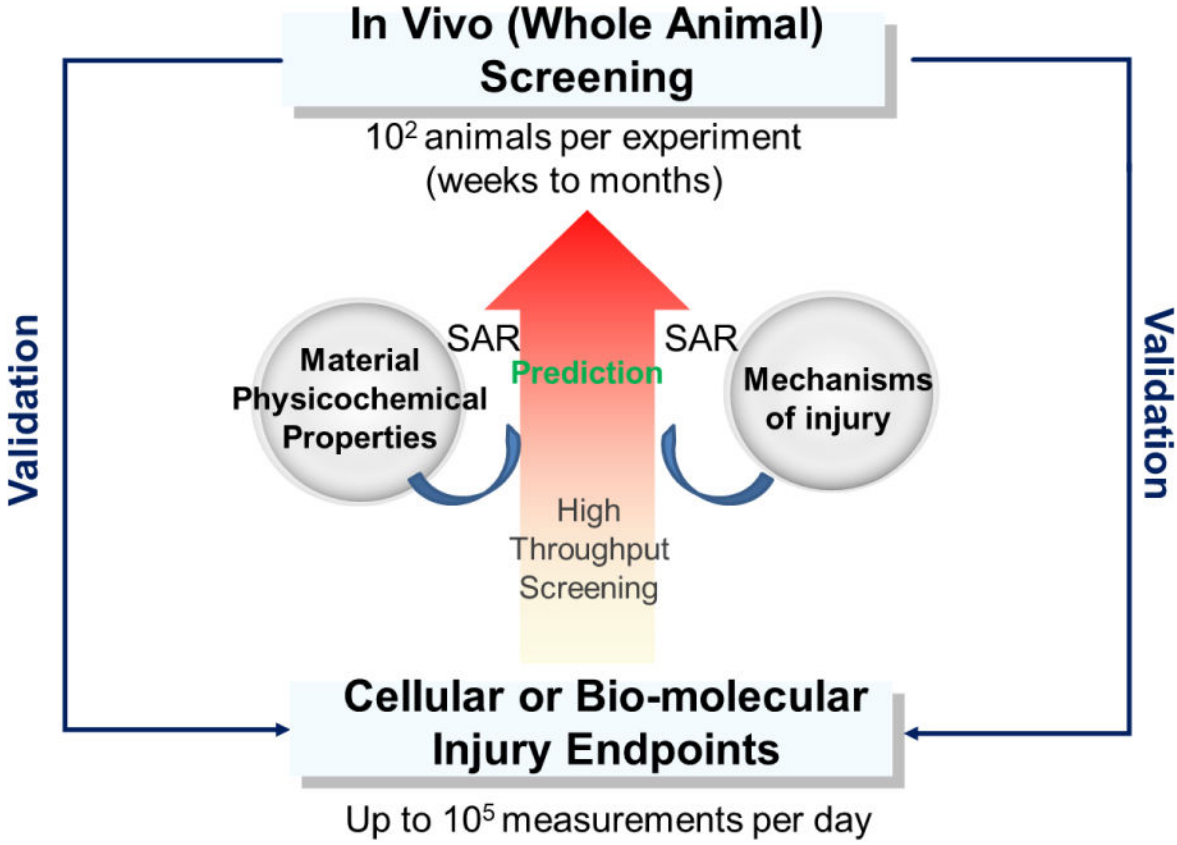

Figure 1.

The predictive toxicological paradigm for ENM hazard testing. A predictive toxicological approach involves establishment of mechanisms of injury related to ENM physicochemical properties. This approach includes establishment of ENM libraries with variations in their physicochemical properties, in vitro ·cellular or bio-molecular injury endpoints of large batches of ENMs using high throughput screening technique. Limited but focused in vivo animal studies are used to validate this in vitro screening method as being ‘predictive’. The quantitative structure-activity relationships (SAR) could be established through data analysis.

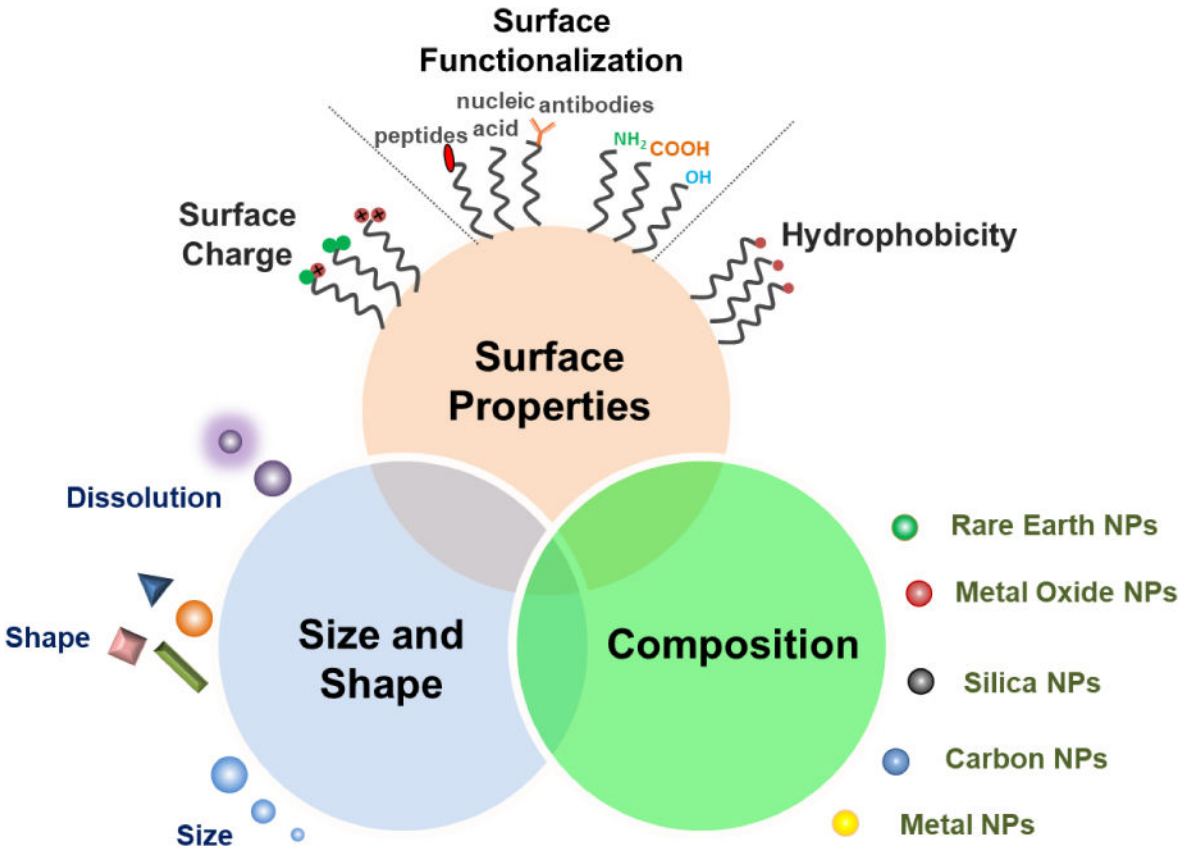

Figure 2.

Examples of ENM libraries. Based on the major physicochemical properties, ENM libraries are built by varying or altering the physicochemical properties. Property variations include chemical composition, size, shape, dissolution, charge, hydrophobicity, surface functional groups, etc. ENM libraries are critical to understand the link between physicochemical properties and toxicity, which allows the development of structure activity relationships.

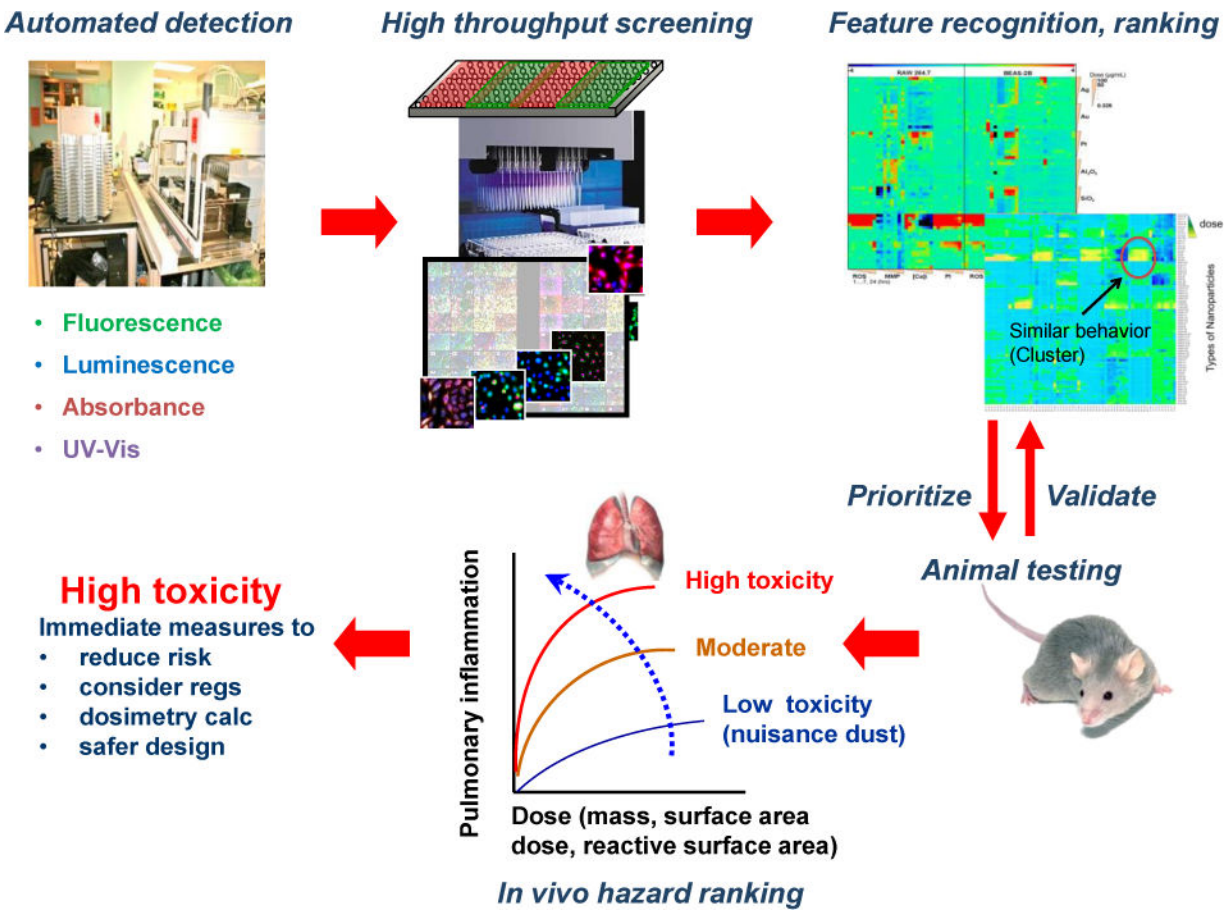

Figure 3.

Multi-parametric HTS analysis by various automated detection strategies (e.g. fluorescence, luminescence, absorbance or UV-Vis etc.) in combination with in silico tools for data analysis and modeling, showing that the in vitro screening approaches can be used for quantitative hazard ranking and development of SARs. Combined with in vivo tests, the HTS assays allow us to establish predictive toxicology paradigms.

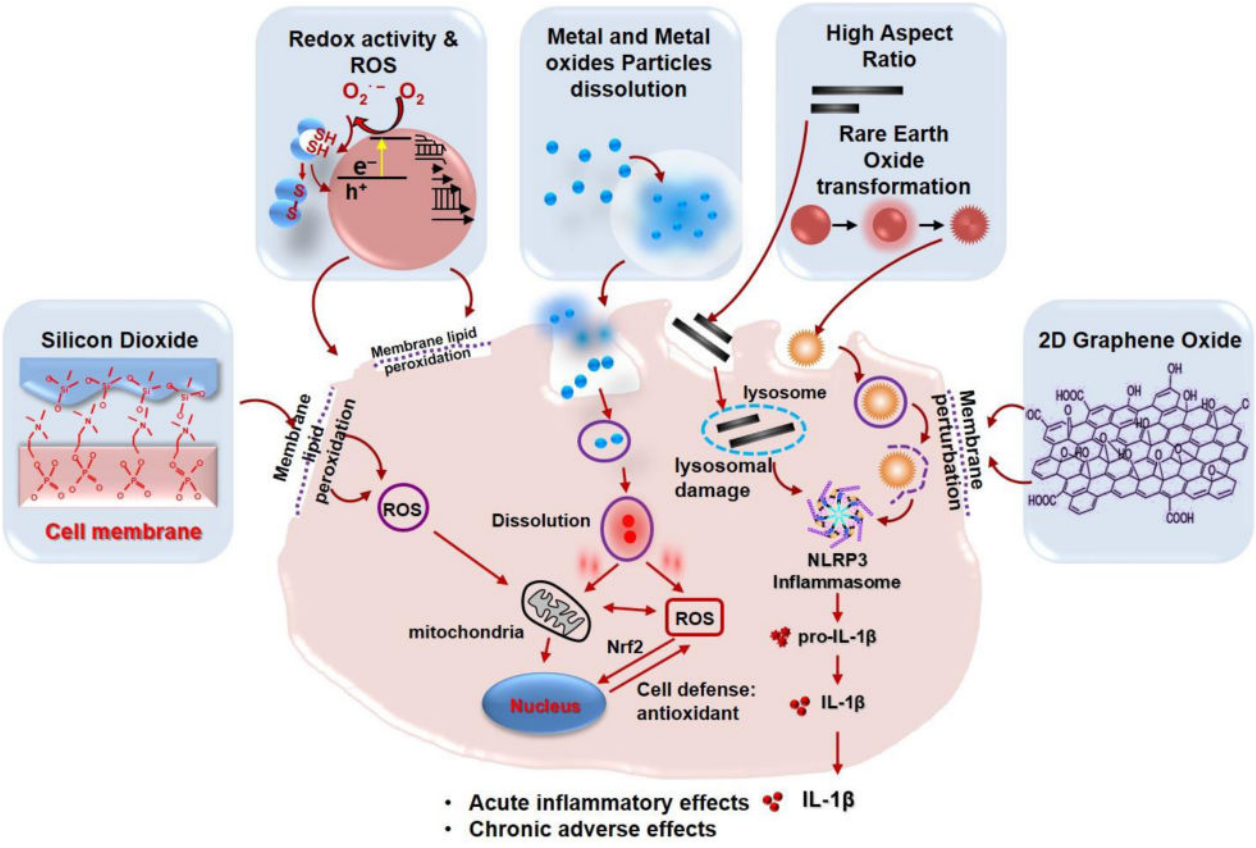

Figure 4.

Examples of mechanistic injury responses for HTS, including metal oxide nanomaterials, silica-based nanomaterials, carbon nanotubes, graphene oxide, and rare earth oxide.

Table 1

Physicochemical characterizaiton of nanomaterials and relevant analytical techniques.

Category of Properties	Specific Physicochemical Properties	Analytical Techniques
Intrinsic	Primary size, shape, size distribution	TEM, SEM, AFM, NTA
	Chemical composition, purity/impurity	EDS, ICP-MS, AAS, Ramen, NMR, FTIR, XPS, TGA
	Aggregate size and fractal structure	TEM, SAXS, DLS
	Pore size, porosity, surface area	BET, SAXS
	Crystallinity, crystal size, framework structure	XRD, Raman, SAXS, NMR
	Roughness, chemical heterogeneity	AFM, FTIR, XPS, NMR, Raman
	Elemental speciation, redox state	EDX, Raman, NMR
	Electronic, magnetic, photonic properties	UV-Vis, EPR, Raman, SAXS
Extrinsic	Endotoxin	UV-Vis
	Agglomerate size, size distribution, agglomeration kinetics	DLS, UV-Vis
	Surface (zeta) potential, isoelectric point	Zeta potential
	Dissolution rate	ICP-MS, UV-Vis
	Hydrophobicity partitioning	UV-Vis
	Sedimentation and dispersion kinetics	UV-Vis
	ROS production	EPR, UV-Vis, Fluorescence probes
Toxicity relevant properties	Band energies of semiconductor materials	UV-Vis, XPS
	Aspect ratio	TEM, SEM, AFM
	Adsorption of phosphate on REO particles	ICP-MS, EDX, XRD
	Carbon radicals on graphene oxide	EPR, UV-Vis
	Silanol and siloxane concentration on silica	Raman, FTIR, BET

TEM: transmission electron microscopy, SEM: scanning electron microscopy, AFM: atomic force microscopy, NTA: nanoparticle tracking analysis, EDS: energy dispersive spectroscopy, ICP-MS: inductively coupled plasma mass spectroscopy, AAS: atomic absorption spectroscopy, Raman: Raman spectroscopy, NMR: nuclear magnetic resonance, FTIR: Fourier transform infrared spectroscopy, XPS: X-ray photoelectron spectroscopy, TGA: thermal-gravimetric analysis, SAXS: small angle X-ray scattering, DLS: dynamic light scattering, BET: Brunauer-Emmett-Teller surface area analysis, XRD: X-ray diffraction, UV-Vis: UV-Vis spectroscopy, EPR: electron paramagnetic resonance, EDX: Energy-dispersive X-ray spectroscopy. Adapted from Ref. [24].

Table 2

Summary of bioanalytical techniques and assays to assess the biological impact of ENMs on various cells

Endpoints	Example Nanomaterials	Assays/Techniques
Cell viability	Cationic NPs [15], crystalline silica [37]	Single parameter MTS, LDH, and ATP assays; ROS production, calcium flux, mitochondrial depolarization, and plasma membrane leakage [38, 39]
Cell uptake, as well as integrity of phagolysosome function	Graphene oxide [40], 2D- Molybdenum Disulfide [41], polymer-based NPs [42]	Confocal microscopy for fluorescently labeled ENMs, TEM, flow cytometry and the effect of endocytosis inhibitors or siRNA knockdown of major proteins involved in cellular uptake. For metal and metal oxides, ICP-OES [43–45, 41, 46]
Oxidative stress	UFP [47], CNTs [48], metal/metal oxide NPs [49], Cationic NPs [15]	Chemiluminescense and fluorescence assays including GSH-Glo Glutathione Assay, MitoSox Red staining, CellROX red staining, Lipid peroxidation assay, which could be combined with similar assays for cell viability [39, 50, 41]
Pro-inflammatory cytokines	Metal Oxide NPs [49], CNTs [48], UFP [51], long aspect ratio materials [12]	Luminex bead-based multiplex assays, Bio-Plex, ELISA, Cytokine arrays, microarray assays, flow cytometry for IL-6, IL-1β, TNF-α, IL-12, IFN-γ [50, 52]
Anti-inflammatory cytokines	Gold NPs [53], Fullerene [54]	Luminex bead-based multiplex assays, Bio-Plex, ELISA, flow cytometry for IL-10, TGF-β [52, 50]
Lysosomal dysfunction and NLRP3 inflammasome activation	UFP [47], cationic NPs [15], CNTs [48], long aspect ratio materials [12]	Confocal microscopy for Magic Red-Cathepsin B release (LMP), TEM, Confocal or fluorescence microscopy to assess lysosomal pH using pHrodo® dyes; NLRP3 activation determined by IL-1β production, with confirmation of involvement of ASC and NLRP components by siRNA knockdown [50, 21, 55, 56]
Autophagy disruption	Rare earth NPs, Silica NPs [57]	TEM to visualize autophagosome; Confocal microscopy for LC3II immunostaining and lysosome (LAMP1) co-localization; Western blotting for LC3 cleavage; Autophagy inhibitors (3-methyladenine, Wortmannin, Chloroquine) [55]

Table 3

Pro's and con's of representative methods for analyzing cytokines

Methods	Pros	Cons
ELISA	High specificity High sensitivity Wide analytical range Reproducibility	Unable to distinguish between bioactive and inactive molecules Varing binding affinity of antibodies Large sample volume High reagent costs Narrow dynamic range Only one protein measurement at a time Matrix/Hetero-philic (auto-) antibody interference
Protein microarray	Sensitive High throughput Rapid Parallel measurement of multiple proteins	Low protein detection system stability (denaturation) Non-specific activity of capture protein Masking of low protein levels by higher protein levels Matrix/Hetero-philic (auto-) antibody interference
Bead based multiplex immunoassays	High specificity High sensitivity Broad analytical and dynamic range Reproducibility Rapid Small sample volume	Unable to distinguish between bioactive and inactive molecules Matrix/ Hetero-philic (auto-) antibody interference

Adapted from Ref. [75].